uranium atoms per particle is 7.6×10^4. Since the density of UO_2 is 11 g/cm^3, the equivalent diameter of the particle, if it were pure UO_2, would be 18 nm. The statistical error of the number of ^{235}U atoms per particle is ± 100 $[(1/339) + (1/6)]^{1/2} = \pm 41$ percent, which corresponds to a change in the equivalent diameter of -3 to $+2$ nm.

No corrections have been made for the single tracks due to background uranium in the filter or for chance orientation of single tracks from adjacent particles to form an apparent double track. These corrections tend in the same direction so that P_2/P_1 would probably not change sufficiently to produce a significant change in the estimated particle size.

We consider 18 nm a reasonable estimate of the equivalent diameter of average mass of a probably lognormal distribution of Cosmos-954 reactor particles. This compares favorably to the equivalent diameter of average mass of 12 nm observed from the reentry burnup of the ^{238}Pu-fueled SNAP-9A generator in 1964 (*8*).

P. W. KREY, R. LEIFER
Environmental Measurements Laboratory, U.S. Department of Energy, New York 10014
W. K. BENSON
Division of International Security Affairs, U.S. Department of Energy, Washington, D.C. 20585
L. A. DIETZ
H. C. HENDRIKSON, J. L. COLUZZA
Knolls Atomic Power Laboratory, General Electric Company, Schenectady, New York 12301

References and Notes

1. Operation Morning Light, *U.S. Department of Energy Report NV-198* (1978).
2. V. Rich, *Nature (London)* **271**, 497 (1978).
3. M. D. Millionshchibov *et al.*, *Proc. 3rd Int. Conf. Peaceful Uses At. Energy, Geneva* **15**, 146 (1964).
4. J. A. McHugh, *Int. J. Mass Spectrom. Ion Phys.* **3**, 267 (1969).
5. L. A. Dietz, C. F. Pachucki, J. C. Sheffield, A. B. Hance, L. R. Hanrahan, *Anal. Chem.* **32**, 1276 (1960).
6. F. A. White, F. M. Rourke, J. C. Sheffield, *Appl. Spectrosc.* **12**, 46 (1958).
7. L. A. Dietz and H. C. Hendrickson, in *Selected Measurement Methods for Plutonium and Uranium in the Nuclear Fuel Cycle*, R. J. Jones, Ed. (U.S. Atomic Energy Commission, Washington, D.C., 1963).
8. P. W. Krey, *Science* **158**, 769 (1967).
9. R. J. List and K. J. Telegadas, *Atmos. Sci.* **26**, 1128 (1969).
10. "Catalog of standard reference materials," *Nat. Bur. Stand. (U.S.) Spec. Publ. 260* (1970).
11. R. L. Fleischer, P. B. Price, R. M. Walker, *Nuclear Tracks in Solids, Principles and Applications* (Univ. of California Press, Berkeley, 1975).
12. We are grateful to P. H. McDonald, J. F. Stevens, and C. F. Pachucki for mass spectrometer measurements; W. H. Howe for statistical consultation; J. A. Bistline, Jr., and C. E. Sanborn, Jr., for neutron irradiations in the KAPL thermal test reactor; and the Air Force Geophysics Laboratory and Physical Science Laboratory of New Mexico State University for the balloon flights.

20 March 1979; revised 15 June 1979

Remote Detection of Biological Stresses in Plants with Infrared Thermometry

Abstract. *Green leaves of mature sugar beets infected with* Pythium aphanidermatum *and cotton infected with* Phymatotrichum omnivorum *had midday radiant leaf temperatures 3° to 5°C warmer than adjacent plants with no sign of disease. The temperature difference persisted under varying conditions of soil moisture and could be used to detect biological stress imposed by these soilborne root-rotting fungi.*

Remote sensing technology is rapidly emerging as a useful tool in the early detection of crop stresses for optimum agricultural resource management. Water stress, perhaps the most ubiquitous of all crop stresses, has also proved one of the most readily identifiable by remote techniques. Plants that have been subject to limited amounts of water exhibit higher leaf temperatures than those with an ample water supply (*1*). We have exploited this phenomenon by using infrared thermometry to detect water stress and to predict its ultimate effect on crop yield and water requirements (*2*).

Other types of crop stress that interfere with water uptake by plant roots or the translocation of water to the leaves for evaporation, or both, should also be amenable to previsual detection and characterization. Intrigued by this possibility, we initiated several experiments to assess the potential of infrared thermometry (*3*) to detect biological stresses imposed by two different soilborne fungal diseases. The first was a root-rot disease of mature sugar beets (*Beta vulgaris* L.), caused by *Pythium aphanidermatum* Edson (Fitz.) (*4*); the second was a root-rot disease of cotton (*Gossypium* sp.), caused by *Phymatotrichum omnivorum* (Shear) Dug. (*5*).

We used hand-held infrared thermometers (*6*) to measure radiant leaf temperatures of sunlit green leaves on plants in several commercial fields of sugar beets (south of Phoenix) and cotton (Marana, Arizona) where a relatively high incidence of the two fungal diseases had been confirmed. Next, we pulled each plant from the soil with as much of its root system as possible, and, based on the macroscopic appearance of the roots, two observers assigned to it a disease category as follows: (i) healthy plants with no evidence of disease; (ii) slightly diseased plants showing early signs of fungal infection (in sugar beets, lesions were evident on the root surface but less than 10 percent of the root volume was damaged; in cotton, the vascular structures of the root were discolored), and (iii) moderately diseased plants exhibiting more advanced symptoms of the disease (in sugar beets, we defined this class as those plants having 10 to 60 percent of the root volume destroyed; in cotton, we found that roots were decaying, the cortex was sloughing off, and the main root was covered with a network of fungal mycelia).

Our results (Table 1) revealed that the radiant leaf temperatures of moderately diseased sugar beets averaged 2.6° to 3.6°C warmer than those of healthy plants, yet we were unable to ascertain disease incidence visually without examining the roots. In subsequent visits to the same fields, we found that healthy sugar beets always remained cooler than moderately diseased plants despite progressively drier soil conditions which resulted in higher plant temperatures. In fact, by 6 July, all plants were wilting from obvious water stress, yet differences in the leaf temperature between diseased and healthy plants persisted. It was not possible to distinguish between healthy and slightly infected sugar beets either visually or with leaf temperature data. We interpreted these results to mean that a certain minimum volume or critical region of the root needed to be affected by the fungus before water uptake or translocation became impaired. Plants in which *P. aphanidermatum* had destroyed more than 60 percent of the root were conspicuous and easy to identify without root inspection. In these plants all the leaves were dead and either yellow or brown with radiant temperatures ranging between 50° and 60°C, usually slightly warmer than adjacent sunlit soils.

Our results with cotton infected with *P. omnivorum* were similar. Slightly diseased plants were not significantly warmer than healthy individuals, nor could we identify them visually without inspecting the roots. Sunlit green leaves on moderately diseased plants, however, averaged 3.3° to 5.3°C hotter than those on plants with no sign of fungal infection. The temperature difference was evident even on 18 August, 1 day after an irrigation, when aboveground visual clues to infection (that is, wilting) were not reliable. We did observe that, as soil moisture was depleted, the moderately diseased plants invariably wilted first. In fact, on 24 August, all these plants had wilted and, even though their foliage re-

0036-8075/79/0810-0585$00.50/0

Table 1. Mean leaf temperatures ± 1 standard error of sugar beet and cotton plants classified according to the degree of root damage by *P. aphanidermatum* and *P. omnivorum*. Data were collected in south central Arizona during 1978 from live green leaves. Sample size is given in parentheses. Ambient air temperatures and vapor pressures were calculated from an aspirated psychrometer positioned 1 m above the soil surface. Data were normalized as discussed in the text.

Date	Time (M.S.T.)	Radiant leaf temperatures (°C)			Ambient air temperature (°C)	Vapor pressure (mbar)
		Healthy noninfected plants	Slightly diseased plants	Moderately diseased plants		
		Sugar beets				
19 June	1120–1230	31.5 ± 0.36 (27)	31.5 ± 3.35 (3)	34.5 ± 1.13 (5)	37.3	18.5
29 June	1200–1400	33.1 ± 0.49 (11)	32.4 ± 2.00 (2)	35.7 ± 1.46 (5)	35.9	18.9
6 July	1200–1400	38.5 ± 0.41 (33)	37.6 ± 0.80 (7)	42.1 ± 0.52 (13)	38.6	7.5
Normalized to 33.1°C and combined		33.1 ± 0.20 (71)	33.1 ± 0.89 (12)	36.1 ± 0.54 (23)		
		Cotton				
18 August	1104–1145	29.3 ± 0.29 (21)	37.5 ± . . . (1)	32.9 ± 1.03 (8)	32.0	24.3
18 August	1215–1228	31.2 ± 0.34 (15)	30.9 ± 0.82 (6)	36.5 ± 1.03 (9)	33.9	22.7
24 August	0930–1000	29.2 ± 0.51 (13)	31.0 ± 0.97 (13)	33.0 ± 1.02 (16)	30.2	24.5
24 August	1100–1114	29.2 ± 0.13 (28)	30.2 ± 0.40 (9)	34.1 ± 0.85 (3)	31.2	24.5
24 August	1440–1448*	30.5 ± 0.57 (5)	29.9 ± . . . (1)	33.8 ± 1.08 (4)	35.0	20.2
Normalized to 29.2°C and combined		29.2 ± 0.13 (82)	30.5 ± 0.53 (30)	33.4 ± 0.52 (40)		

*Data for this time period only were from pima cotton (*Gossypium barbadense* L.). The remaining cotton data were from deltapine cotton (*G. hirsutum* L.).

mained green, they were easily distinguished both visually and thermally from turgid healthy plants.

Mean temperatures within a disease category were quite variable from one experimental period to the next because of changes in available soil moisture and microclimate. Thus, to make the sugar beet data for three separate days more comparable and to be able to combine them, we normalized each temperature to 33.1°C, which was the mean temperature of healthy plants on 29 June. This required adding 1.6°C to measurements of healthy and diseased plants observed on 19 June (1.6°C is the difference between the mean healthy plant temperatures on 19 and 29 June). Likewise, we subtracted 5.4°C from each observation on 6 July because healthy plants on that day averaged 5.4°C warmer than those on 29 June. Cotton temperatures during each experimental period were normalized to 29.2°C in a similar fashion. The results (Table 1, rows labeled "Normalized and combined") indicate that the transformation maintained separability between the extreme classes while compensating for the widely differing soil moisture and environmental conditions encountered during each time. It also increased our sample size, enabling us to generate normal Gaussian frequency distributions (*7*) for visualization of class separability based on radiant leaf temperatures (Fig. 1, A and B). The temperature distributions of healthy and moderately diseased plants were not totally exclusive (*8*). Nevertheless, when we used the temperature at the crossover point of the two distributions to classify our original normalized data, we found that it predicted whether an individual plant was diseased significantly better than expected by chance alone (*9*).

For example, we found that 27 percent of the sugar beets had normalized leaf temperatures above 34.6°C, leading us to believe that they were moderately diseased; the actual disease incidence was 22 percent. Based on a temperature discriminator of 31.0°C, we would have estimated that 30 percent of the cotton plants were infected; we observed 26 percent moderately diseased plants. When evaluating disease incidence in a mixed population of plants, we expected good agreement between predicted and observed values since compensating errors in classification cancel each other out. However, we discovered that a relatively small proportion of healthy plants (18 percent of sugar beets, 7 percent of cotton) were erroneously classified as moderately diseased. Conversely, a percentage of truly diseased plants (39 percent of sugar beets, 25 percent of cotton) were wrongly predicted to be healthy. These misclassifications may be the result of variables that were not accounted for in our study, such as undiagnosed disease or abiotic stresses, genetic variability, and differences in microhabitat or root penetration. In addition, we suspected that many of the moderately diseased plants tolerated the fungi without reducing evapotranspiration. Since the predicted and observed disease incidence was linearly correlated in our study, it may, after substantiation through additional independent field observation, offer a method whereby predictions could be adjusted to more closely match actual conditions.

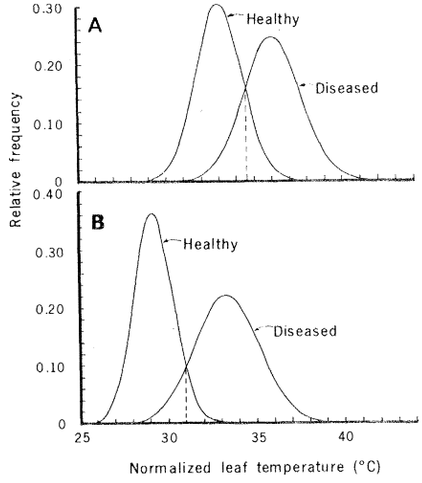

Fig. 1. Gaussian frequency distributions of normalized and combined leaf temperature data for healthy and moderately diseased (A) sugar beets and (B) cotton, showing the extent of overlap and the temperatures (dashed line) proposed as a discriminator between the two classes.

Our results demonstrate the utility of infrared thermometry in detecting two soilborne fungal diseases of sugar beets and cotton. The fundamental principles will probably prove applicable to many other types of biological and physical plant stresses.

P. J. PINTER, JR.
U.S. Water Conservation Laboratory, Phoenix, Arizona 85040
M. E. STANGHELLINI
University of Arizona, Tucson 85721
R. J. REGINATO, S. B. IDSO
U.S. Water Conservation Laboratory
A. D. JENKINS
Spreckels Sugar Division, Amstar Corporation, Chandler, Arizona 85224
R. D. JACKSON
U.S. Water Conservation Laboratory

References and Notes

1. C. B. Tanner, *Agron. J.* **55**, 210 (1963); D. M. Gates, *ibid.* **56**, 273 (1964); C. L. Wiegand and L. N. Namken, *ibid.* **58**, 582 (1966); W. L. Ehrler, *ibid.* **65**, 404 (1973).
2. S. B. Idso, R. D. Jackson, R. J. Reginato, *Science* **196**, 19 (1977); R. D. Jackson, R. J. Reginato, S. B. Idso, *Water Resour. Res.* **13**, 651 (1977); R. J. Reginato, S. B. Idso, R. D. Jackson, *Remote Sensing Environ.* **7**, 77 (1978); W. L. Ehrler, S. B. Idso, R. D. Jackson, R. J. Reginato, *Agron. J.* **70**, 999 (1978).
3. Infrared photography and infrared thermometry are fundamentally different. Leaf temperatures cannot be recorded with infrared photography because the film is not sensitive to emitted thermal energy [N. L. Fritz, *Photogramm. Eng.* **33**, 1128 (1967)]. Infrared radiation thermometers measure emitted thermal radiation; they thus provide a remote, noncontact means to observe radiant leaf temperatures and infer rates of evapotranspiration. Several earlier studies have demonstrated that infrared thermometry facilitates the identification of biological stress in certain forest and agricultural species [R. C. Heller, *Proc. Symp. Remote Sensing Environ.* **5**, 387 (1968); C. De Carolis, G. Baldi, S. Galli de Paratesi, G. M. Lechi, *ibid.* **9**, 1161 (1974); C. De Carolis, G. G. Conti, G. M. Lechi, *ibid.* **10**, 1219 (1976); C. E. Olson, Jr., *ibid.* **11**, 933 (1977); R. Kumar, L. F. Silva, M. E. Bauer, *Publication N78-29537* (National Technical Information Service, Springfield, Va., 1978)].
4. M. E. Stanghellini and E. L. Nigh, *Plant Dis. Rep.* **56**, 507 (1972); M. E. Stanghellini and J. D. Russell, *Phytopathology* **63**, 133 (1973).
5. R. B. Streets and H. E. Bloss, *Am. Phytopathol. Monogr. 8* (1973); H. E. Bloss and R. B. Streets, Sr., *Prog. Agric. Ariz.* **24**, 8 (1972); C. M. Rush and S. D. Lyda, in *Proceedings of the Beltwide Cotton Production Research Conferences* (National Cotton Council, Memphis, Tenn., 1978), p. 23.
6. For the sugar beets we used a Barnes PRT-5 infrared thermometer with a 2° field-of-view lens; for the cotton we used a Telatemp AG-42 infrared thermometer with a 2.5° field-of-view lens. Both were equipped with a 10.5- to 12.5-μm band-pass filter. Radiant temperatures were not corrected for target emissivity. Trade and company names are included for the benefit of the reader but imply no endorsement or preferential treatment of the product cited by the U.S. Department of Agriculture.
7. J. H. Zar, *Biostatistical Analysis* (Prentice-Hall, Englewood Cliffs, N.J., 1974), p. 70.
8. The frequency distributions of slightly diseased plants are not shown in Fig. 1, A and B, because they were essentially coincident with that of healthy plants.
9. We compared observed versus predicted disease incidence for healthy and moderately diseased categories, using 2×2 χ^2 contingency tables (sugar beets, $\chi^2 = 15.3$; cotton, $\chi^2 = 59.2$).

10. We thank T. N. Jordan, W. C. Kronland, and R. S. Seay for technical assistance. Contribution from the Agricultural Research, Science, and Education Administration, U.S. Department of Agriculture, Phoenix, Ariz.; the University of Arizona, Tucson; and the Amstar Corporation, Spreckels Sugar Division, Chandler, Ariz.

15 January 1979; revised 2 April 1979

Enchancement of Luminance Flicker by Color-Opponent Mechanisms

Abstract. *Color-opponent ganglion cells in the monkey retina respond to luminance flicker at high temporal frequencies. Color opponency, which makes these cells so selective of wavelength at low temporal frequencies, is progressively lost at high frequencies. This loss is due to a frequency-dependent phase shift between the responses of spectrally different center and surround mechanisms in the receptive field of each of these cells. Center and surround responses, which are antagonistic at low temporal frequencies, become synergistic at high ones, making these cells most responsive at high frequencies to those wavelengths to which they are least responsive at low frequencies. This phenomenon can explain the differences between chromatic and luminance flicker in human vision.*

Periodic changes in the luminance of a light produce a sensation of flicker. If these changes in luminance are large, flicker can be observed at frequencies as high as 70 to 80 Hz. Flicker can also be observed if the chromaticity (wavelength composition) of a light is varied, while luminance is kept constant. At low frequencies this chromatic flicker is more effective than luminance flicker but at high frequencies the converse is true (*1*, *2*). The neurophysiological basis for this difference between the perception of luminance and chromatic flicker is unknown. Suggestions have been made (*2*, *3*) that these perceptual differences could be due to the properties of two distinct classes of cells detectable in primate retina (*4*) and lateral geniculate nucleus (*5*): one class, which is wavelength selective (the so-called color-opponent cells), and the other, which does not show color opponency and is consequently selective only for the effective energy of luminance of light.

We have examined this hypothesis in single ganglion cells subserving the central retina of the rhesus monkey. The physiology of one class of cells, the color-opponent variety alone, may provide the entire explanation for the differences between chromatic and luminance flicker functions. Color-opponent cells respond better to chromatic changes at low temporal frequencies and better to luminance changes at high temporal frequencies. This phenomenon is due to a frequency-dependent phase shift between the color-opponent responses produced by the center and surround mechanisms in the receptive field of each of these cells. What are spectrally antagonistic responses at low frequencies become progressively synergistic at high frequencies.

We recorded the extracellular impulses of single ganglion cells in the retina of monkeys (*Macaca mulatta*) anesthetized with sodium pentobarbital (Nembutal, 5 mg per kilogram of body weight per hour, injected intravenously), paralyzed with gallamine triethiodide (Flaxedil, 10 mg kg^{-1} $hour^{-1}$, injected intravenously), and artificially ventilated; CO_2 in the expired air was continuously monitored and kept within the range of 4 to 5 percent. Recordings were made with glass micropipette electrodes filled with 3*M* KCl solutions, which were introduced into the eye through a closed chamber and guided to the retina by a hydraulic micromanipulator under direct vision (with a modified Bausch and Lomb fundus camera). The camera provided a means of presenting visual stimuli in Maxwellian view, which could be seen in sharp focus on the retinal surface (*4*). The light source was a 1000-W xenon arc lamp providing two independent beams. Flickering stimuli with equal periods of light and darkness were produced by a half-sectored disk rotated at a focal point in one beam by a variable-speed motor and monitored continuously by a photocell. The wavelength and energy in this beam were changed by narrow-band interference and neutral density filters, respectively; sharp cut absorption filters (Corning 2408, red; 3482, yellow; and 5543, blue) in the second beam provided selective chromatic adaptation. Fusion and response latencies to increasing flicker frequencies were determined ($\pm$ 1 msec) by superimposing 10 to 20 responses and stimuli on a double-beam storage oscilloscope, which provided a continuous monitor of the phase relationship of the response to the stimulus cycle.

We classified 385 single ganglion cells in the central retina (0° to 12° eccentricity) according to the position of its receptive field center and the cone mechanisms influencing its responses (*6*). The flicker fusion frequencies of 38 cells were studied intensively; 30 of these showed color opponency. In color-opponent cells both center and surround mechanisms in a cell's receptive field could usually be studied separately by an appropriate choice of wavelength. In general, the flicker fusion frequency of all cells increased with the intensity of light stimulation. The highest flicker fusion frequencies were attained by phasic ganglion cells that did not show color opponency. The average flicker fusion frequency of phasic cells was 62 Hz [$N = 8$, standard deviation (S.D.) = 11]. In the parafoveal retina, where such phasic cells are common, color-opponent cells also follow high flicker frequencies. Those whose receptive field centers were mediated by the red cone mechanism had an average maximum flicker fusion frequency of 53 Hz

0036-8075/79/0810-0587$00.50/0